Assessment of α' Phase Precipitation in Neutron-Irradiated Model Fe-Cr-Al Alloys

S.A. Briggs[1], P.D. Edmondson[2], K.G. Field[2], Y. Yamamoto[2], K.C. Littrell[2], K.A. Terrani[2], K. Sridharan[1]

[1]University of Wisconsin-Madison
Madison, WI 53706

[2]Oak Ridge National Laboratory
Oak Ridge, TN 37831

Research Motivation

- Fe-Cr-Al alloys show promise as candidate materials for accident-tolerant fuel (ATF) cladding applications due to their excellent high-temperature corrosion and oxidation resistance
  - Demonstrates superior performance in the steam environments of loss-of-coolant accident (LOCA) conditions when compared to Zr-based alloys currently in service, which tend to exacerbate accidents by oxidizing exothermically and producing H_2 gas[1]
- High-Cr ferritic systems typically face problems with hardening and embrittlement due to dislocation loop formation and α' phase precipitation under LWR-relevant conditions
  - α' precipitation normally occurs after long-term thermal aging in Fe-based alloys with Cr contents over 9 at.% under 475°C[2]
  - Kinetics of precipitation are typically slow - radiation has been shown to accelerate the formation of this phase[3]
- Precipitation in binary Fe-Cr has been extensively studied but it is unclear how Al additions affect this phenomena
  - Understanding how Cr and Al content can be balanced to maintain adequate material properties and corrosion resistance while mitigating deleterious precipitation effects is crucial to designing an ideal candidate alloy optimized for ATF cladding applications

Research Goals

- **Investigate how precipitation response is affected by varying Cr and Al contents**
- **Study evolution of cluster morphology from beginning of life to expected end of life (EOL) radiation dose**
  - EOL dose for LWR fuel cladding is ~16 dpa
- **Correlate precipitation data with mechanical testing results to develop predictive models of embrittlement response**

Experimental

- **Samples**
  - Four Fe-Cr-Al model alloy compositions
  - Fabrication route:
    Arc-melted→heat-treated → hot forged/rolled → cold-rolled (10% reduction)[4]
  - ~20-50μm grain size
- **Irradiation Campaign**
  - Multiple SS-J2 tensile specimens for each composition were loaded into four separate capsules and irradiated in the High-Flux Isotope Reactor (HFIR)
  - Temperature was determined by using passive SiC thermometry techniques

Table 1: *Fe-Cr-Al alloy compositions in wt.%*

Alloy	Fe	Cr	Al	Y	C	Si
Fe-10Cr-4.8Al	bal.	**10.01**	4.78	0.038	0.005	<0.01
Fe-12Cr-4.4Al	bal.	**11.96**	4.42	0.027	0.005	0.01
Fe-15Cr-3.9Al	bal.	**15.03**	3.92	0.035	0.005	0.01
Fe-18Cr-2.9Al	bal.	**17.51**	2.93	0.017	0.005	<0.01

**S, O, N, and P contents at or below 10 ppm*

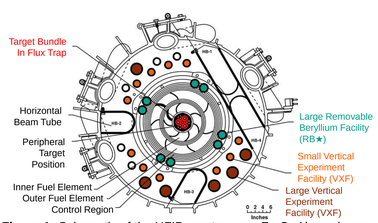

Figure 1: *Schematic of the HFIR reactor core. Fe-Cr-Al specimens were irradiated in the central flux trap.*

Table 2: *Irradiation conditions for each irradiation capsule in HFIR*

Capsule ID	Exposure Time (hrs)	Neutron Flux (n/cm²s) E > 0.1 MeV	Neutron Fluence (n/cm²) E > 0.1 MeV	Dose Rate (dpa/s)	Dose (dpa)	Irradiation Temperature (°C)
FCAY-01	120	**8.54×10^{14}**	**3.69×10^{20}**	**7.7×10^{-7}**	0.3	334.5±0.6
FCAY-02	301	**8.54×10^{14}**	**9.25×10^{20}**	**7.7×10^{-7}**	0.8	355.1±3.4
FCAY-03	614	**8.84×10^{14}**	**1.95×10^{21}**	**8.1×10^{-7}**	1.8	381.9±5.4
FCAY-04	2456	**8.74×10^{14}**	**7.73×10^{21}**	**7.9×10^{-7}**	7.0	319.9±10.2

Atom Probe Tomography Analysis

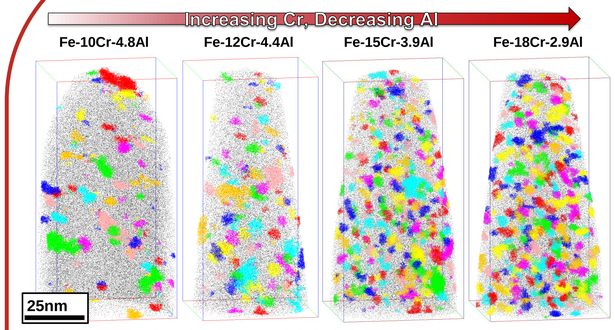

Figure 2: *Comparison of precipitate morphologies in the four Fe-Cr-Al compositions irradiated to 7 dpa at 320°C. α' precipitates indexed by the cluster finding algorithm are uniquely colored. Black atoms represent 2% of the detected Fe atoms; regions-of-interest are 50×50×100 nm*

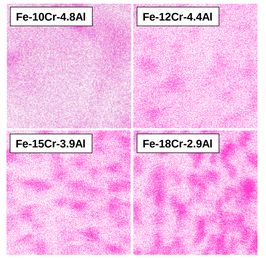

Figure 3: *40×40×20 nm Cr atom map for each of the four Fe-Cr-Al compositions irradiated to 7 dpa at 320°C*

α' precipitates are observed as spheroidal Cr-rich clusters and are found in all irradiated specimens

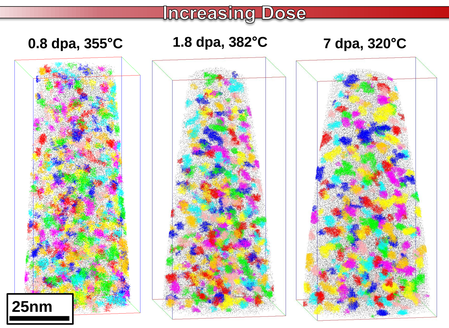

Figure 4: *Comparison of precipitate morphologies in Fe-18Cr-2.9Al irradiated to 0.8, 1.8 and 7 dpa. Note that there is some variation in the actual irradiation temperature due to the nature of in-core neutron radiation experiments. α' precipitates indexed by the cluster finding algorithm are uniquely colored. Black atoms represent 2% of the detected Fe atoms; regions-of-interest are 50×50×100 nm*

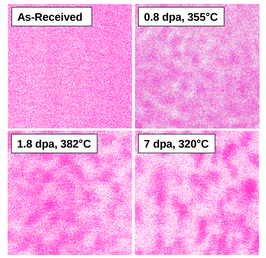

Figure 5: *40×40×20 nm Cr atom map for the various dose conditions studied for Fe-18Cr-2.9Al*

Small Angle Neutron Scattering Analysis

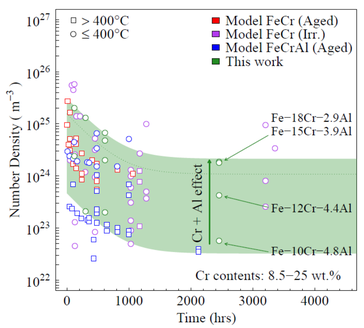

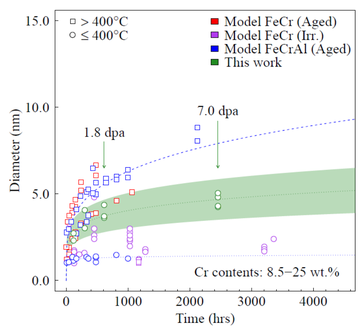

Figure 6: *Comparison of SANS results with those found in literature. Green data points are from the current study. SANS analysis assumes spherical clusters with composition Fe-81.3Cr-4.7Al (wt.%) interacting with an exclusion volume. Established trends from aged Fe-Cr-Al alloys are indicated by blue lines[5]. All other data points compiled from various sources[6]*

- Trends in SANS data indicate that cluster number density decreases and cluster size increases with increasing dose
- Additionally, increasing Cr content results in a higher number density of precipitates
- In qualitative agreement with APT results in this study and with published literature

Discussion

- Clusters are observed in all irradiated Fe-Cr-Al specimens and the severity of the precipitation response increases with dose and increasing Cr content
- Cr content of α' clusters in Fe-Cr-Al range from ~50-62 at.% - much lower than the ~85 at.% clusters observed in binary Fe-Cr
  - Al is seen to be rejected from the α' phase (not shown)
  - Suggests that Al additions shift the α-α' phase boundary
- Cluster morphology appears to be approaching saturation by 7 dpa
  - Increasing dose results in cluster coarsening as number density decreases and cluster size increases

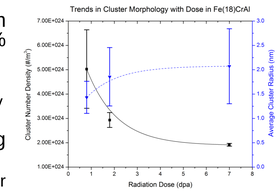

Figure 7: *Observed dose trends for precipitate morphologies in Fe-18Cr-2.9Al*

Table 3: *Summary of results of cluster analysis for all Fe-Cr-Al alloys studied at 7 dpa. Compositions are given in at.%*

	Matrix Composition			Average Cluster Composition			Number Density	Volume Fraction	Average Radius
Alloy	Fe	Cr	Al	Fe	Cr	Al	($\times 10^{24}$ m^{-3})	(%)	(nm)
Fe-10Cr-4.8Al	80.99	9.26	9.54	44.39 ± 6.17	50.14 ± 7.02	5.32 ± 1.81	0.51	2.41	1.65 ± 0.99
Fe-12Cr-4.4Al	80.69	10.61	8.57	45.10 ± 5.09	49.49 ± 5.43	5.26 ± 1.19	0.69	3.94	1.95 ± 0.90
Fe-15Cr-3.9Al	80.30	11.91	7.60	39.21 ± 5.44	56.01 ± 5.76	4.64 ± 1.15	2.2	7.93	1.76 ± 0.70
Fe-18Cr-2.9Al	80.61	13.13	6.02	34.82 ± 4.46	61.44 ± 4.70	3.58 ± 0.82	1.9	10.20	2.07 ± 0.77

Conclusions

- **Precipitation response is sensitive to alloy composition and irradiation conditions**
  - ↑ in Cr ∝ ↑ in α' num. density & ↑ in α' diameter
  - ↑ in dpa ∝ ↓ in α' num. density & ↑ in α' diameter

  } Hardening response will vary with composition and dose – needs to be investigated
- **Al additions result in a significant change in α' cluster composition**
  - Could result in precipitates being a weaker barrier to dislocation motion – reduced hardening contribution
- **Cluster morphologies appears to be nearly saturated by 7 dpa**
  - Neutron irradiation to this dose is likely sufficient to gauge radiation-response in these alloys
- **Alloy composition must be optimized to enhance radiation tolerance**
  - Correlation with mechanical testing results and hardening models is still in progress

Future Work

- **Assess end-of-life cluster morphologies**
  - Fifth Fe-Cr-Al irradiation capsule to 16 dpa available for analysis
  - Confirm saturation of precipitation and mechanical properties
- **Analyze mechanical properties and build dispersed barrier hardening models to evaluate structure/property relationships**
  - Allows for predictive modeling of radiation response
- **Investigate effects of other minor solute elements**
  - Final commercial alloy for cladding applications will likely contain Mo for solid solution strengthening, in addition to increased impurities
  - Selection of alloys for future irradiation experiments will be based off of the results of this study

Acknowledgements

Research was sponsored by the U.S. DOE's Office of Nuclear Energy, Advanced Fuel Campaign of the Fuel Cycle R&D Program and the U.S. DOE's Office of Science, Fusion Energy Sciences. Research on the CG-2 General Purpose SANS at ORNL's HFIR was sponsored by the Scientific User Facilities Division, Office of Basic Energy Sciences, U.S. DOE and research on the Cameca LEAP 4000X HR housed at the Center for Advanced Energy Studies (CAES) and ORNL was sponsored by the National Scientific User Facility (NSUF) and the Center for Nanomaterials Science (CNMS), respectively.

References

[1] B.A. Pint, et al., *Journal of Nuclear Materials* **440**, 420 (2013).
[2] G. Bonny, D. Terentyev, & L. Malerba, *Scripta Materialia* **59**, 1193 (2008).
[3] M.H. Mathon, et al., *Journal of Nuclear Materials* **312**, 236 (2003).
[4] Y. Yamamoto, et al., *Journal of Nuclear Materials* **467**, 703 (2015).
[5] S. Messoloras, et al., *Metal Science* **18**, 311 (1984).
[6] See Refs. 26; 30-32; and 38-42 in K.G. Field, et al. *ORNL Technical Report*, ORNL/TM-2015/518 (2015).